Journal of Organometallic Chemistry, 413 (1991) 269–286
Elsevier Sequoia S.A., Lausanne
JOM 21732

Evidence for correlated rotation and diastereoisomer discrimination in (η^4-diene)Fe(CO)$_2$L complexes: the crystal and solution structures of (cyclohexadiene)Fe(CO)$_2$P(*o*-tolyl)$_3$ and (cycloheptadiene)Fe(CO)$_2$(+)-PPh$_2$(neomenthyl) *

James A.S. Howell *, Michael G. Palin, Marie-Claire Tirvengadum
Chemistry Department, University of Keele, Keele, Staffordshire ST5 5BG (UK)

Desmond Cunningham, Patrick McArdle
Chemistry Department, University College, Galway (Ireland)

Zeev Goldschmidt and Hugo E. Gottlieb
Chemistry Department, Bar Ilan University, Ramat-Gan 52100 (Israel)

(Received December 17th, 1990)

Abstract

The solid state structure of (cyclohexadiene)Fe(CO)$_2$P(*o*-tolyl)$_3$ reveals an *exo*$_2$ conformation for the phosphine. In solution, arene ring exchange in the phosphine and exchange of phosphine between equivalent basal positions of the square pyramid occur at equal rates. In solution, (cycloheptadiene)Fe(CO)$_2$(+)-PPh$_2$(neomenthyl) exhibits a diastereoselection between basal isomers, and crystallizes as a single diastereoisomer which has been structurally characterized.

Introduction

Tertiary phosphines form the largest class of commonly encountered ancillary ligands in organotransition metal complexes and provide great potential for the control of structure and reactivity through variation of both steric and electronic properties. Of particular relevance to catalysis are the ability of demanding ligands such as P(*o*-tolyl)$_3$ to promote coordinative unsaturation [1,2] and the ability of homochiral bidentate phosphines to control enantioselectivity [3]. In many complexes, both phosphine and a π-bound ene or polyene ligand occupy positions in the metal co-ordination sphere. Though restricted rotation is a common feature of many ene and polyene complexes [4], and though restricted M–PR$_3$ rotation has been

* Dedicated to Professor Peter Pauson on the occasion of his retirement.

0022-328X/91/$03.50

observed (albeit rarely) [5], we are aware of no example where correlated or "gear" rotation (defined as a conformational transmission caused by interaction between polyhedral substituents) has been confirmed experimentally in a (polyene)$M(PR_3)$ complex [6,7], though correlated rotation has been observed in many organic systems [8].

We present here evidence for possible correlated rotation in (η^4-cyclohexadiene)$Fe(CO)_2P(o\text{-tolyl})_3$ and the conformational diastereoselection resulting from introduction of homochiral (+)-PPh_2(neomenthyl) into symmetric (diene)$Fe(CO)_3$ complexes. Such complexes continue to attract attention as synthetic intermediates, particularly for enantioselective synthesis [9].

Results and discussion

Complexes **1**, **2a,b** and **3** were prepared by substitution of the tricarbonyl in the presence of Me_3NO [10]. Spectroscopic data are given in Table 1.

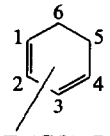

$Fe(CO)_2P(o\text{-tolyl})_3$

(1)

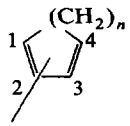

$Fe(CO)_2PPh_2$(neomenthyl)

(2a: $n = 2$; **2b**: $n = 3$)

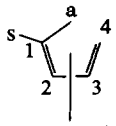

$Fe(CO)_2PPh_2$(neomenthyl)

(3)

(a) Crystal and solution structure of (cyclohexadiene)$Fe(CO)_2P$(o-tolyl)$_3$ (1)

Though single crystal studies of $P(o\text{-tolyl})_3$ and the series $XP(o\text{-tolyl})_3$ (X = O, S, Se) have been reported [11], we are not aware of any structural study of a transition metal complex of $P(o\text{-tolyl})_3$. The structures of **1** and of (cyclohexadiene)-$Fe(CO)_2PPh_3$ [12] are displayed in Fig. 1. Structural data (Table 2) show similar pseudo-square pyramidal geometries with phosphine in a basal position. Minimization of interaction of $P(o\text{-tolyl})_3$ with the sterically most demanding C3–C8 region of the diene is evident in an increased M–P distance, an increased C2–Fe–P angle, and an increased tilting of the diene (manifest in increased Fe–C3,6 and decreased Fe–C4,5 distances). Of most interest is the conformation of the $P(o\text{-tolyl})_3$ ligand, termed exo_2, in which the plane of one ring is essentially collinear with the Fe–P axis and the methyl points away from the phosphorus lone pair. Such a conformation is also found for $XP(o\text{-tolyl})_3$ (X = S, Se) [11], though $OP(o\text{-tolyl})_3$ and the free ligand itself adopt a conformation in which all three methyls reside on the same side as the lone pair (termed exo_3). The literature cone angle value is based on this conformation [13]. Modelling studies show that the exo_2 conformation reduces the cone angle of the ligand substantially from 184 to 160° [14*]. The PPh_3 ligand in (cyclohexadiene)$Fe(CO)_2PPh_3$ also adopts a similar conformation in which the plane of one ring is essentially collinear with the Fe–P axis. This is not, however, common to all (diene)$Fe(CO)_2PPh_3$ structures; the opposite extreme is represented by (*trans,trans*-hexa-2,4-diene)$Fe(CO)_2PPh_3$, which with axial phosphine and C_α–Cp–P–Fe angles of 81, 44 and 25°, presents the face of one phenyl ring (essentially

* Reference number with an asterisk indicates a note in the list of references.

Table 1

NMR spectroscopic data

Complex	Temperature (°C)	^{1}H [a]	^{13}C [b]	^{31}P [c]
1	+20	1,4 2.63 (br) [e]	1,4 57.6 (br) [e]	46.0 [e]
		2,3 4.24 (br)	2,3 89.1 (br)	
		5,6(*exo*) 1.41 (d)	5,6 24.4	
		5,6(*endo*) 1.88 (d)		
		Me 2.10 (br)	Me 23.2 (4.0)	
		Ph 6.9–7.8 (m)	Ph 125–143	
	−50	1,4 2.25 (m)	1,4 [d]	46.0
		2.70 (m)	61.9 (6.1)	
		2,3 3.20 (m)	2,3 85.6	
		5.20 (m)	94.1	
		5,6(*exo*) 1.30 (m)	5,6 23.6	
			24.1 (5.4) [e]	
		5,6(*endo*) 1.85 (dd)	Me 22.5 (6.1)	
			22.8 (5.3)	
		Me 1.28 (s)	23.2 (2.2)	
		2.23 (s)	Ph 125–143	
		2.53 (s)	CO 216.5 (20.8)	
		Ph 6.5–9.0 (m)	223.3 (6.7)	
2a	+20 [h]	1,4 2.36 (m) [f]	1,4 60.3 (2.9) [e]	72.3 [e]
		2.72 (m)	61.1 (2.1)	
		2,3 4.40 (m)	2,3 85.8	
		4.53 (m)	86.2	
		5,6 g	5,6 24.4	
			24.9	
			CO 219.8 (12.4)	
			219.7 (14.6)	
2b	+20 [h]	1,4 2.57 (m) [f]	1,4 54.8 (3.8) [e]	70.6 [e]
		2,3 3.72 (m)	58.0	
		4.55 (m)	2,3 87.9	
		5–7 g	91.4	
			5,7 28.4	
			28.7	
			6 24.6	
			CO 220.7(10.7)	
			218.2 (15.7)	
3	+20 [h]	1,4a −0.40 (m) [f]	1,4 41.1 [e]	74.4 [e]
		1,4s 1.32 (m)	41.8	
		2,3 4.52 (m)	2,3 85.2	
		4.80 (m)	85.8	
			CO 217.4 (7.8)	
			217.9 (6.9)	
SeP(*o*-tolyl)$_3$	+20	Me 2.31 (s) [e]	Me 23.1 (4.4) [e]	26.4 (712) [i]
		Ph 7.2–7.7 (m)	C1 128.2 (72.9)	
			C2 143.0 (8.8)	
			C3–C6 126.2 (12.7)	
			132.0 (2.9)	
			132.9 (10.3)	
			134.1 (13.2)	
	−100	Me 1.61 (s)	Me 20.8 (6.3)	

Table 1 (continued)

Complex	Temperature (°C)	^1H [a]	^{13}C [b]	^{31}P [c]
$SeP(o\text{-tolyl})_3$		2.24 (s)	23.8 (3.4)	
		2.82 (s)	24.6 (3.2)	
		Ph 6.8–9.0 (m)	Cl–C6 124–144	
	−110			28.8
				(699) [i]
				23.7
				(699)

[a] ppm from TMS. [b] ppm from TMS; J(C–P) in parentheses. [c] ppm from 85% H_3PO_4; J(P–Se) in parentheses. [d] Under solvent resonance. [e] CD_2Cl_2 solution. [f] C_6D_6 solution. [g] Under menthyl resonance (1.1–1.9). [h] Resonances due to (+)-PPh_2(neomenthyl) = (^1H) 6.9–7.9 (Ph); 0.34 (Me, J = 7.1); 1.03, 1.07 ($CHMe_2$, J = 7.1); 1.0–3.0 (ring). (^{13}C) 17.1, 20.4, 21.3 (11.7), 24.0, 28.0 (5.8), 28.8, 30.3 (3.9), 31.0 (6.8), 38.9 (20.5), 39.7 (3.9), 127–139 (Ph). Complexes **2b** and **3** exhibit similar values. [i] CD_2Cl_2/Et_2O (1:1) solution.

perpendicular to the Fe–P axis) to the acyclic diene [16]. Other (diene)$Fe(CO)_2PPh_3$ complexes, both axially and basally substituted, adopt intermediate conformations [16,17].

The low temperature limiting ^{13}C and ^1H spectra of **1** (Table 1) are consistent with the solid state structure, exhibiting axial and basal carbonyl resonances, six resonances for the C_6 ring, and three methyl resonances for the $P(o\text{-tolyl})_3$ ligand. At higher temperature, two distinct fluxional processes are observed, namely exchange of phosphine between equivalent basal positions and exchange of the three non-equivalent *o*-tolyl rings. These processes are most easily analysed by line shape analysis [18] of the CH_2(diene) and CH_3 ^{13}C resonances respectively; observed and calculated spectra are shown in Fig. 2. The substantial change in chemical shift of the methyl resonances as a function of temperature may be noted; P–C coupling for the CH_2 resonances is best fitted with low temperature values of 2.1 Hz (unresolved) and 5.4 Hz of *opposite* sign which yield a coupling of 1.5 Hz (again unresolved) at +20°C. The derived $\Delta G^{\ddagger}$ values [19*] (Table 3) are equivalent. Similarly, the less precise $\Delta H^{\ddagger}$ and $\Delta S^{\ddagger}$ values overlap at the 95% confidence level [19*]. Simple coincidence seems unlikely; we have observed a similar process in (η^4-tropone)$Fe(CO)_2P(o\text{-tolyl})_3$ [22] in which lack of high temperature limiting spectra prevented the type of detailed analysis reported here, and basal-basal exchange in (cyclohexadiene)$Fe(CO)_2PPh_3$ remains fast on the NMR time scale at −90°C [16].

To aid in the interpretation of these results, we have also examined methyl exchange in $SeP(o\text{-tolyl})_3$, an exo_2 molecule [11] which is not complicated by the additional asymmetry of the basal (diene)$Fe(CO)_2P$ moiety. In both ^{13}C and ^1H spectra (Fig. 3), the single room temperature methyl resonance is broadened and resolved at low temperature into the three resonances expected for the exo_2 isomer. Line shape analysis of the ^1H spectra shows clearly an equivalent collapse of the three resonances with $\Delta H^{\ddagger} = 8.8 \pm 0.3$ kcal mol^{-1} and $\Delta S^{\ddagger} = 2.9 \pm 1$ cal K^{-1} mol^{-1} [23]. Though resonances attributable to the exo_3 isomer are not observed in the ^1H spectra at low temperature, a small population of this isomer is evident in the low temperature ^{31}P spectrum (Fig. 3) in which two resonances of unequal intensity

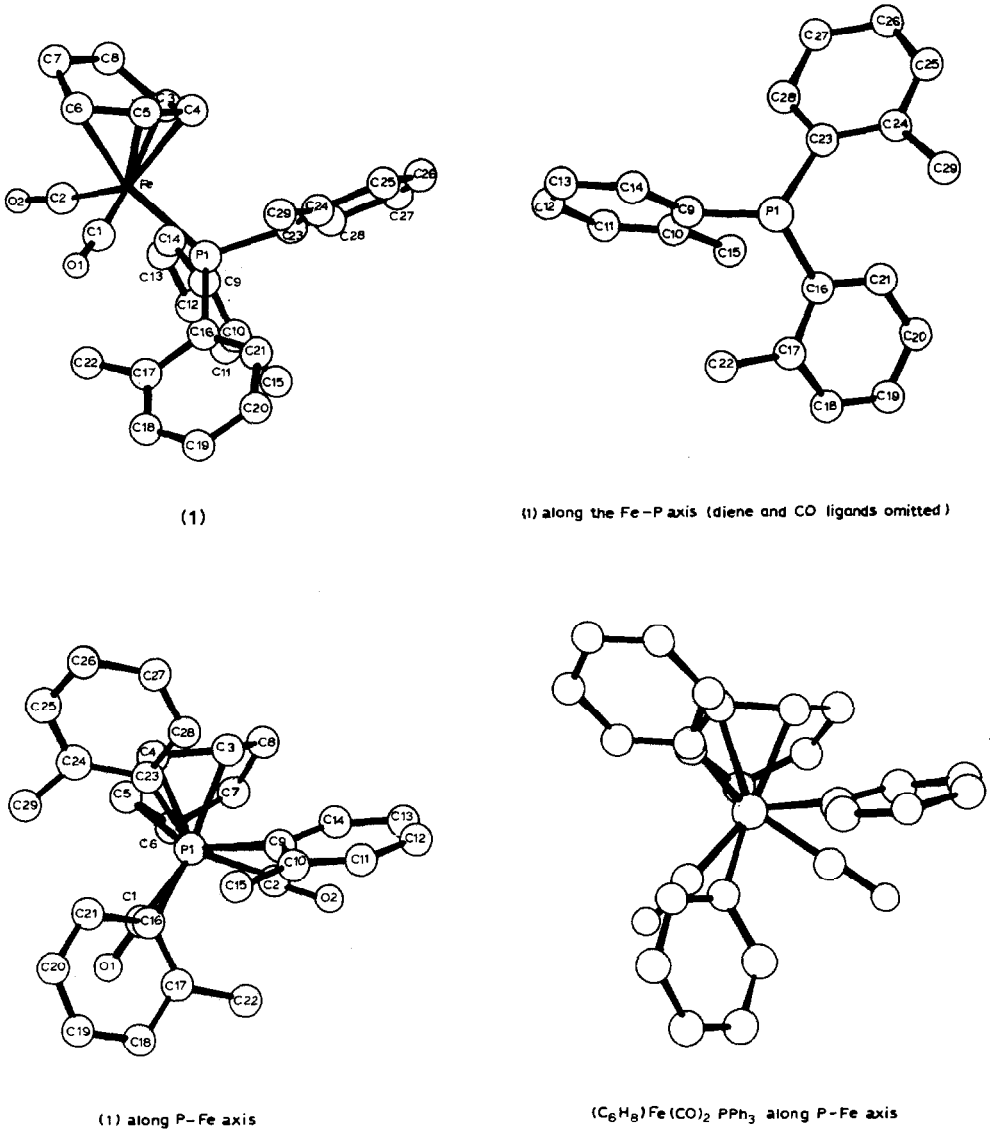

Fig. 1. Molecular structure of **1** and $(C_6H_8)Fe(CO)_2PPh_3$ (hydrogen atoms omitted).

(ratio 30 : 1) which both exhibit $^{31}P-^{77}Se$ satellites are observed. The ^{31}P spectrum of **1** is temperature invariant, indicating population of only the *exo*$_2$ isomer.

The permutations of P–C rotational isomerism via ring-flip mechanisms in XAR_3 molecules of this type have been extensively analysed by Mislow and coworkers [8a,24]. Interconversion of *exo*$_2$ and *exo*$_3$ diastereoisomers can occur via the two-ring-flip (Scheme 1) which is the stereomutation mechanism with the lowest energy requirement [25]. Interconversion of the residual enantiomerism (not evident in an achiral medium) requires a higher energy one-ring-flip pathway.

Complete methyl averaging in **1** requires that both P–C and Fe–P bond rotation are fast on the NMR time scale. The low temperature limiting spectra indicate both

Table 2

Selected structural parameters

	1	$(C_6H_8)Fe(CO)_2PPh_3$ [a]	2b	
Fe–C3	2.141(6)	2.11	Fe–C6	2.128(12)
Fe–C4	2.048(6)	2.06	Fe–C5	2.085(15)
Fe–C5	2.042(6)	2.05	Fe–C4	2.058(16)
Fe–C6	2.120(6)	2.10	Fe–C3	2.141(15)
Fe–C1	1.763(6)	1.77	Fe–C1	1.755(16)
Fe–C2	1.761(7)	1.75	Fe–C2	1.765(16)
C1–O1	1.150(6)	1.14	C1–O1	1.171(16)
C2–O2	1.150(7)	1.15	C2–O2	1.143(16)
C3–C4	1.413(7)	1.41	C5–C6	1.436(21)
C5–C6	1.400(7)	1.41	C3–C4	1.385(20)
C4–C5	1.396(7)	1.41	C4–C5	1.401(19)
C3–C8	1.518(7)	1.53	C6–C7	1.540(19)
C6–C7	1.504(7)	1.52	C3–C9	1.523(19)
C7–C8	1.516(7)	1.52	C7–C8	1.498(19)
Fe–P	2.284(2)	2.23	C9–C8	1.499(21)
			Fe–P	2.244(3)
Fe–C1–O1	175.3(6)	175.3	Fe–C1–O1	179 (1)
Fe–C2–O2	175.2(6)	175.2	Fe–C2–O2	173 (1)
C3–C4–C5	115.1(6)	114.9	C4–C5–C6	120 (1)
C4–C5–C6	116.3(6)	114.9	C3–C4–C5	122 (1)
C5–C6–C7	120.8(6)	119.9	C4–C3–C9	126 (1)
C4–C3–C8	119.1(5)	120.5	C5–C6–C7	123 (1)
C6–C7–C8	110.8(5)	110.4	C9–C8–C7	114 (1)
C3–C8–C7	111.8(5)	110.9	C6–C7–C8	115 (1)
			C7–C8–C9	114 (1)
C2–Fe–C1	99.9(3)	101.7	C2–Fe–C1	103.1(7)
C2–Fe–P	102.7(2)	98.7	C2–Fe–P	100.6(4)
C1–Fe–P	93.3(2)	91.7	C1–Fe–P	90.7(4)
Fe–P–C9	117.4(2)	118.8	Fe–P–C10	117.7(4)
Fe–P–C16	114.3(2)	115.0	Fe–P–C16	116.8(4)
Fe–P–C23	113.6(2)	114.0	Fe–P–C22	109.8(4)
Z–Fe–P [b]	123.4	123.4	Z–Fe–P [b]	123.0
Z–Fe–C1	119.1	118.2	Z–Fe–C1	117.8
Z–Fe–C2	119.1	118.0	Z–Fe–C2	117.0
C3–C4–C5–C6	1.1	0.1	C3–C4–C5–C6	3.6
C4–C5–C6–C7	−42.4	−44.1	C4–C5–C5–C7	−58.4
C5–C4–C3–C8	41.6	43.7	C5–C4–C3–C9	54.2
Intraligand parameters				
P–C9	1.849(5)	1.85	P–C10	1.837(14)
P–C16	1.857(6)	1.86	P–C22	1.855(12)
P–C23	1.851(6)	1.85	P–C16	1.875(11)
(C–C) ring(av)	1.39	1.39	(C–C) ring(av)	1.38
C–Me(av)	1.51			
C9–P–C16	102.9(3)	103.0	C10–P–C22	104.4(5)
C9–P–C23	102.4(2)	100.1	C10–P–C16	105.4(6)
C16–P–C23	104.7(2)	103.8	C16–P–C22	100.8(5)
Fe–P–C9–C14	19.2	8.6	Fe–P–C10–C15	20.1
Fe–P–C16–C17	62.4	50.5	Fe–P–C22–C27	−75.5
Fe–P–C23–C24	57.9	51.9		
			C16–C17	1.575(16)
			C17–C18	1.515(17)

Table 2 (continued)

1	$(C_6H_8)Fe(CO)_2PPh_3$ [a]	2b	
		C18–C19	1.579(22)
		C19–C20	1.461(22)
		C20–C21	1.566(19)
		C21–C16	1.525(17)
		C18–C28	1.535(24)
		C21–C30	1.554(19)
		C29–C30	1.468(21)
		C31–C30	1.515(22)
		C16–C17–C18	109 (1)
		C17–C18–C19	112 (1)
		C18–C19–C20	114 (1)
		C19–C20–C21	116 (1)
		C20–C21–C16	108 (1)
		C21–C16–C17	114 (1)
		P–C16–C17	114.0(9)
		P–C16–C21	115.0(8)
		C28–C18–C17	113(1)
		C28–C18–C19	115(1)
		C30–C21–C16	119(1)
		C30–C21–C20	114(1)

[a] Generated by CHEM-X from the data of reference 12. [b] Z is the centroid of the C4 diene system.

slow basal exchange of phosphine and slow P–C bond rotation, but are consistent with either slow or fast Fe–P bond rotation. The former seems most probable, since otherwise it is difficult to reconcile the very substantial effect of the $P(o\text{-tolyl})_3$ on the barrier to diene–Fe rotation; in (cyclohexadiene)$Fe(CO)_2PPh_3$, where no intraligand restricted rotation is observed, basal–basal exchange remains fast on the NMR time scale at $-90\,°C$ [16].

One possible scenario for a correlated rotation in **1** is presented in Scheme 2. The exchange process is initiated by a two-ring-flip mechanism which yields the higher energy exo_3 conformer **A** with inversion of helical chirality. At this point, one may note the enantiomeric relationship between **B** and **B′**; the helical chirality of **A** is therefore mismatched with that of the ground state **B** [27]. It is suggested that complete methyl averaging via P–Fe rotation occurs by gearing which also results in basal–basal phosphine exchange. The requirement for an isoenergetic transition state **A′** also indicates an additional inversion of helical chirality on transit between **A** and **A′** which may be accomplished in a single step via a three-ring-flip mechanism [28*]. One may note at the proposed energy maximum in Scheme 2 the

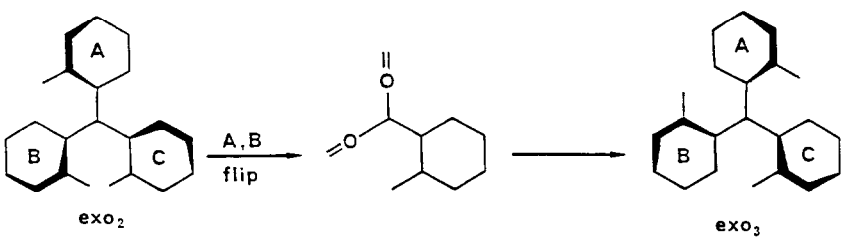

Scheme 1

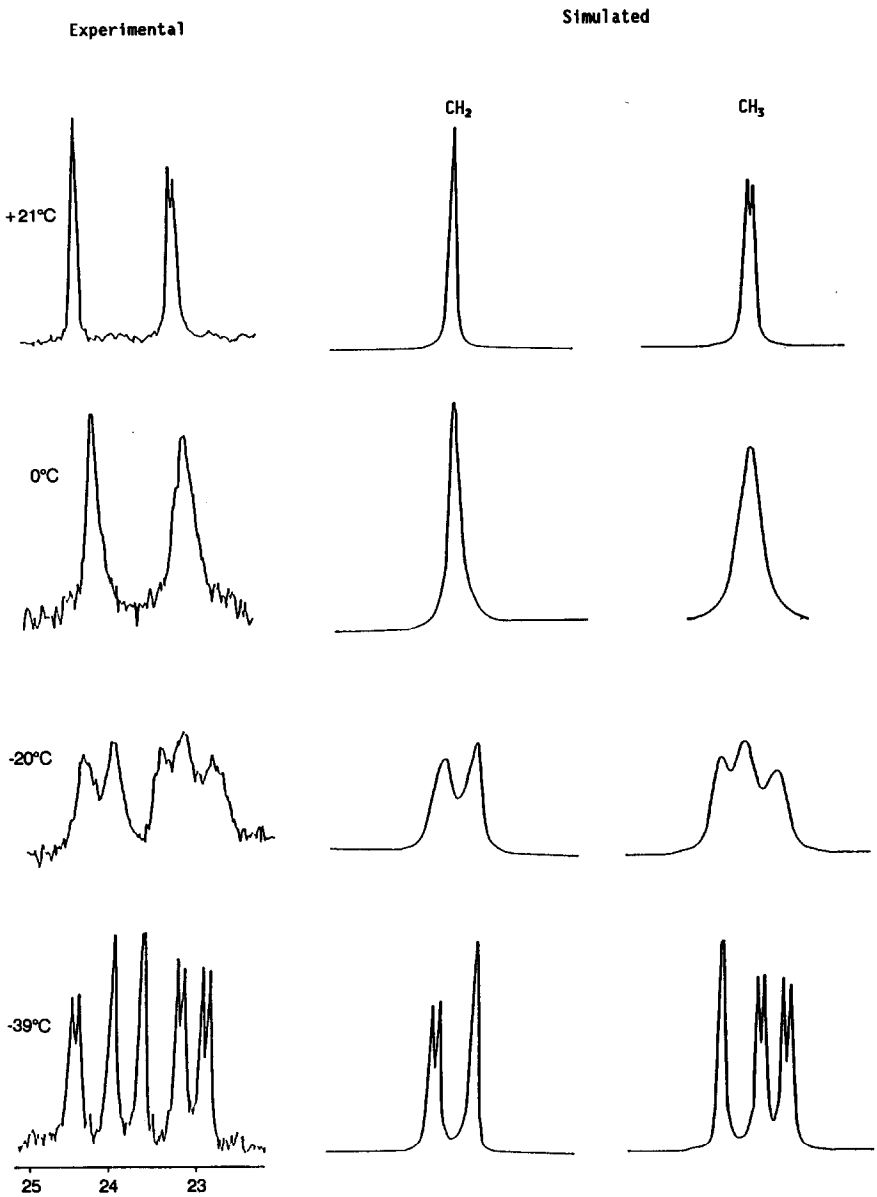

Fig. 2. Observed and simulated ^{13}C NMR spectra for **1**.

superposition of achiral transition states for both basal–basal phosphine exchange and ring (methyl) exchange.

We are currently examining rotational isomerism in other metal carbonyl tri-*o*-tolylphosphine complexes.

*(b) Solution and crystal structure of (cycloheptadiene)Fe(CO)$_2$(+)-PPh$_2$-(neomenthyl) (**2b**)*

The results described above raise the possibility of diastereoisomer discrimination in symmetric (diene)Fe(CO)$_2$L complexes incorporating sterically demanding ho-

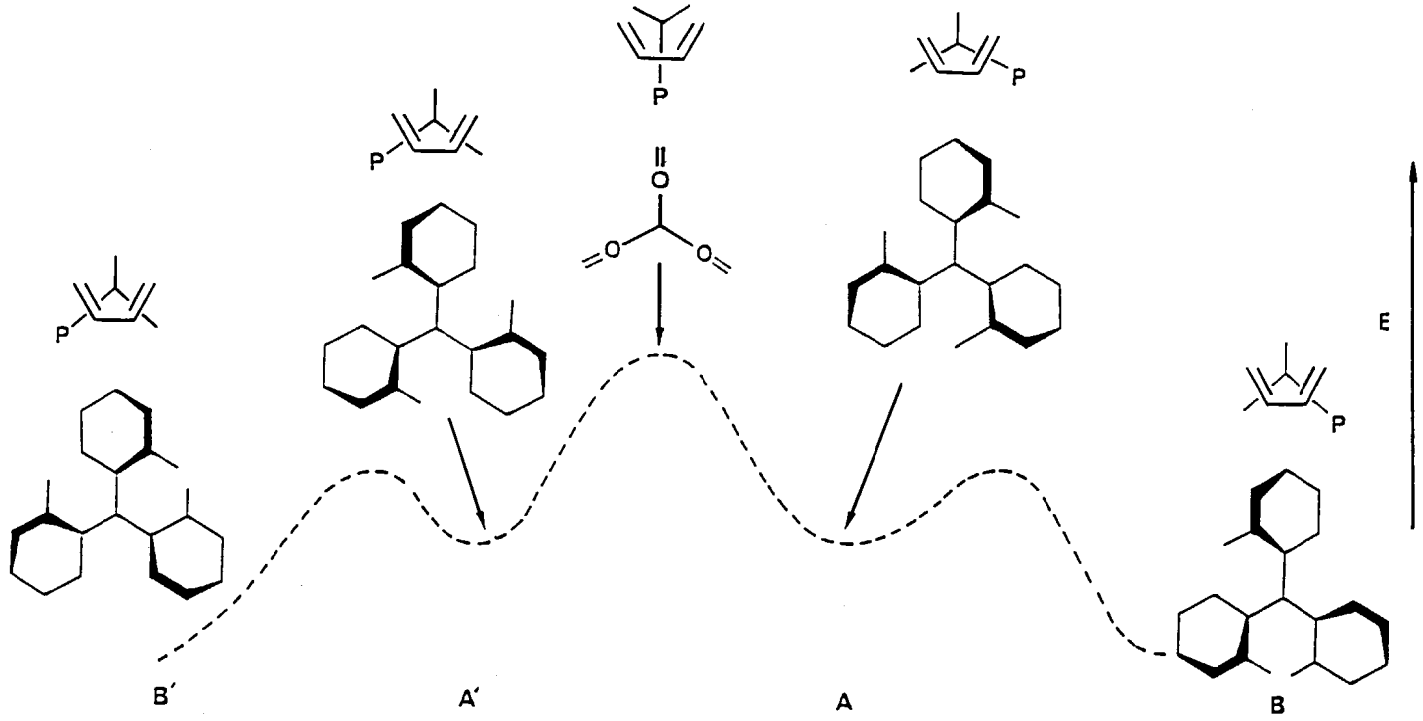

Scheme 2. Energy profile for correlated rotation.

Table 3

Rate constants and $\Delta G^{\ddagger}$ values for CH_2 [a] and CH_3 [b] exchange

T (K)	CH_2		CH_3	
	k (s^{-1})	$\Delta G^{\ddagger}$ (kcal mol^{-1})	k (s^{-1})	$\Delta G^{\ddagger}$ (kcal mol^{-1})
233.8	5 ± 2	12.8 ± 0.3	1.8 ± 0.7	12.8 ± 0.3
243.7	15 ± 5	12.9 ± 0.2	4.5 ± 0.9	12.9 ± 0.2
253.2	30 ± 6	13.0 ± 0.2	19 ± 4	12.7 ± 0.2
267.2	80 ± 16	13.1 ± 0.2	50 ± 10	12.8 ± 0.2
273.6	220 ± 44	13.0 ± 0.2	115 ± 23	12.8 ± 0.2
293.8	1000 ± 400	13.2 ± 0.3	1000 ± 400	12.5 ± 0.3

[a] CH_2: $\Delta H^{\ddagger} = 11.7 \pm 0.8$ kcal mol^{-1}; $\Delta S^{\ddagger} = -5 \pm 3$ cal K^{-1} mol^{-1}. [b] CH_3: $\Delta H^{\ddagger} = 13.8 \pm 1.7$ kcal mol^{-1}; $\Delta S^{\ddagger} = +4 \pm 6$ cal K^{-1} mol^{-1}.

mochiral phosphines. This phenomenon is best demonstrated in the case of **2b**; the single room temperature ^{31}P resonance broadens and resharpens into two resonances at −84°C (Fig. 4) in the ratio 2.5:1 which are assigned to the now non-equivalent diastereoisomer pair **B** and **B′**. The ^{13}C spectrum similarly shows two axial/basal resonance pairs at −84°C averaged to a single pair at room temperature [29]. The complex crystallizes from petroleum ether as a single diastereoisomer in the $P2_12_12_1$ space group common to many homochiral compounds. The molecular structure (Fig. 5) shows that viewed down the diene–Fe axis, the solid state absolute configuration has a right handed [P, CO(axial), CO(basal)] sequence. Structural parameters within the (diene)$Fe(CO)_2P$ polyhedron are similar to those of (cyclohexadiene)$Fe(CO)_2PPh_3$. The diene ligand adopts the boat configuration predicted by solution NMR work [30] and the bending angle at the terminal diene carbons is characteristically larger than in the C_6 complex (56 vs. 44°). One may also note a change in ligand conformation on complexation. While NMR data [31] indicate an axial/equatorial/equatorial conformation for the PPh_2/Me/^{i}Pr substituents in (+)-PPh_2(neomenthyl), the structure of **2b** shows an equatorial/axial/axial arrangement. This configuration is common to other (diene)Fe [32] and (arene)M (M = Cr, Ru) complexes [33] containing (+)-PPh_2(neomenthyl), though the sterically less demanding (+)-PMe_2(neomenthyl) retains the axial/equatorial/equatorial conformation in its *trans*-$NiCl_2L_2$ complex [34].

Other complexes exhibit similar behaviour (Fig. 4). Thus, the ^{31}P spectrum of (cyclohexadiene)$Fe(CO)_2$-(+)-PPh_2(neomenthyl) (**2a**) is partially resolved into two resonances at −80°C in the approximate ratio 1.4:1, while the spectrum of (butadiene)$Fe(CO)_2$-(+)-PPh_2(neomenthyl) exhibits three resonances at −80°C in the ratio 1.6:1:1. The largest is assigned to the axially substituted isomer on the basis of previously observed chemical shift differences for the axial–basal pair of (butadiene)$Fe(CO)_2PPh_3$ [16]. The results thus indicate an essentially equal population of the basal diastereoisomeric pair. Below −80°C, further broadening of the asterisked resonances occurs, indicating the possible onset of restricted P–C or Fe–P rotation.

The chemical consequences of this type of diastereoselection in (diene)$Fe(CO)_2L$ and the related (diene)$Fe(CO)_2LX$ salts are significant. Such a phenomenon may explain the diastereoselectivity observed in the reaction of CN^- with [(cyclohexa-

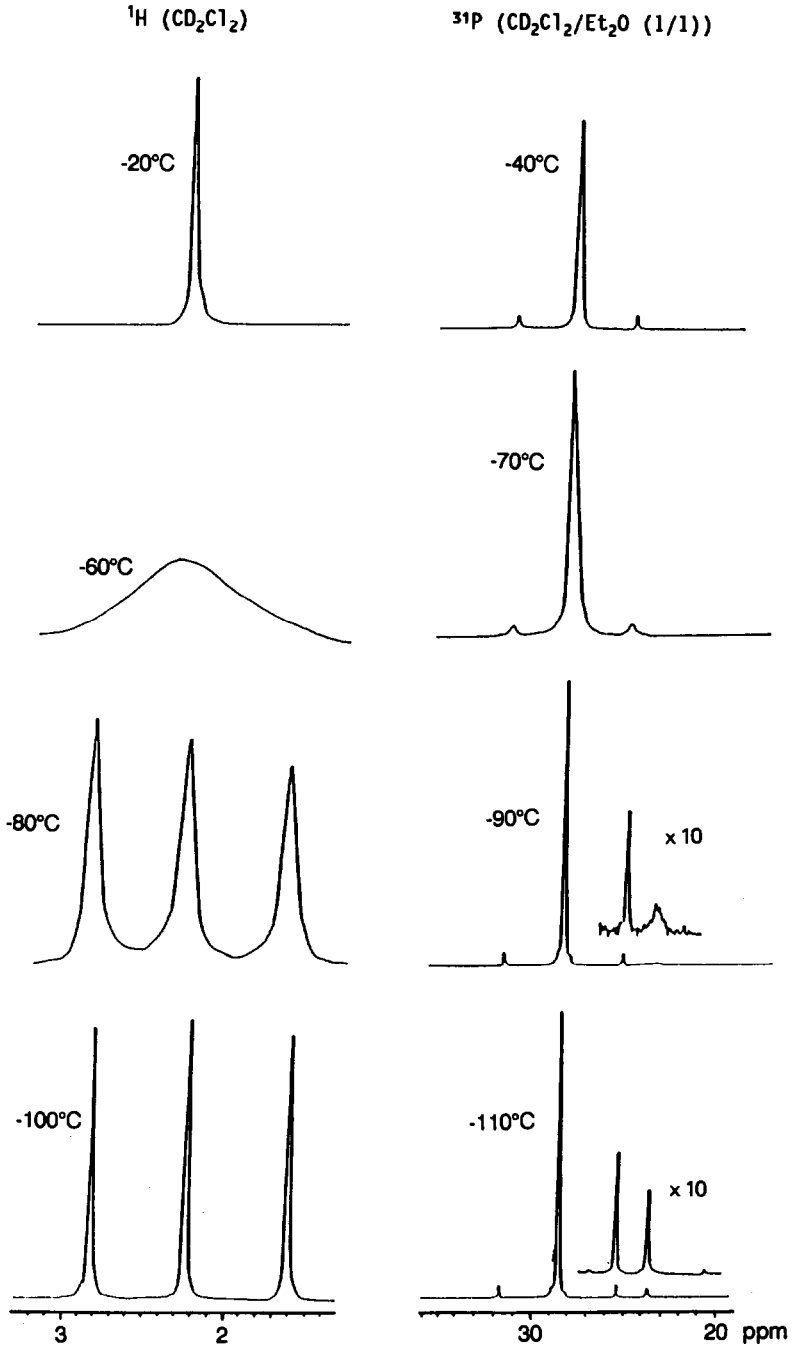

Fig. 3. ^1H and ^{31}P NMR spectra of SeP(*o*-tolyl)$_3$.

dienyl)Fe(CO)$_2$(+)-PPh$_2$(neomenthyl)]PF$_6$ [35], and we are currently examining other sterically demanding homochiral ligands in terms of improving the diastereoselection.

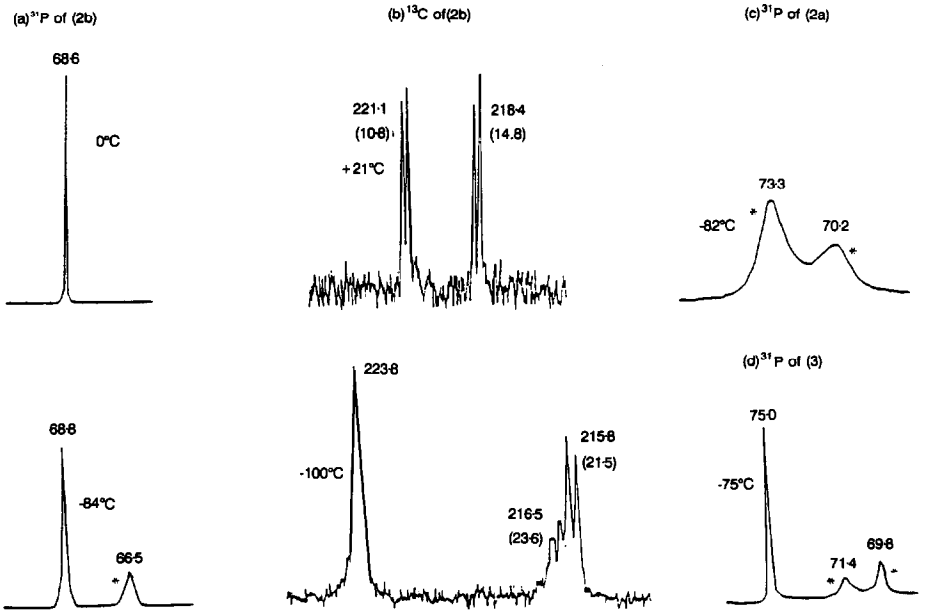

Fig. 4. Variable temperature NMR spectra for compounds 1–3.

Experimental

NMR spectra were recorded on a JEOL GSX-270 spectrometer; temperatures were measured using the in-built copper-constantin thermocouple. (Butadiene)-$Fe(CO)_3$ was purchased; $(C_6H_8)Fe(CO)_3$, $(C_7H_{10})Fe(CO)_3$ [36] and (+)-PPh_2(neomenthyl) [37] were prepared by literature methods. $SeP(o\text{-tolyl})_3$ was prepared by the literature method [38] and recrystallized from ethanol.

(a) Preparation of (cycloheptadiene)Fe(CO)$_2$(+)-PPh$_2$(neomenthyl) (2b)

Me_3NO (3.5 g, 31.5 mmol) was added to a stirred solution of (cycloheptadiene)$Fe(CO)_3$ (4.0 g, 17.1 mmol) and (+)-PPh_2(neomenthyl) (6.5 g, 20.1 mmol) in acetone (100 ml). The mixture was vigorously stirred and heated at reflux with further additions of Me_3NO until the infrared spectrum showed little tricarbonyl remaining. Diethyl ether (150 ml) was added to the cooled mixture which was filtered and evaporated to leave a yellow solid. This residue was redissolved in diethyl ether (50 ml) and stirred with excess MeI to remove unreacted (+)-PPh_2(neomenthyl). After evaporation of solvent the residue was extracted with 5% ethyl acetate–petroleum ether (30–40) and chromatographed on aluminia using the same solvent mixture as eluant. Evaporation of solvent from the yellow band collected gave the product **2b** as a yellow solid (4.1 g, 51%) which was crystallized from petroleum ether (30–40).

Complexes **1**, **2a** and **3** were obtained by a similar procedure. Analytical data for the complexes **1–3** and for $SeP(o\text{-tolyl})_3$ are given in Table 4.

While **2a** may be purified by sublimation (130 °C/0.01 mmHg), **3** decomposes slightly to liberate free phosphine under these conditions and was characterized by accurate mass spectroscopy.

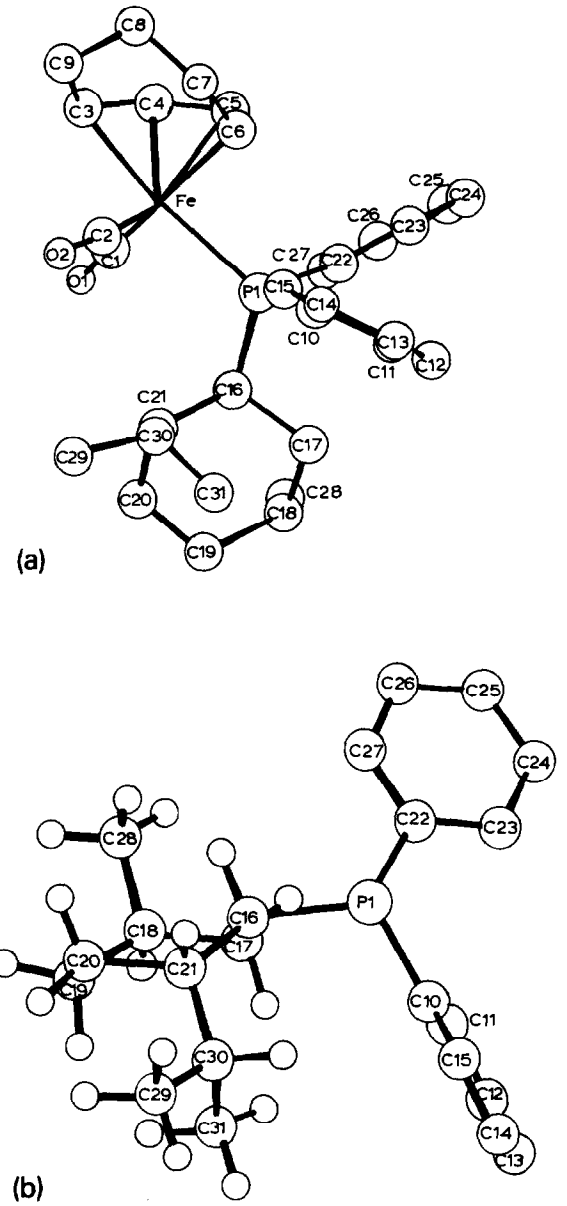

Fig. 5. Molecular structure of **2b**; (a) hydrogen atoms omitted and (b) (+)-PPh_2(neomenthyl) ligand.

(b) Crystal data

Data for **2b** were collected on a Hilger Watts Y290 diffractometer using Mo-K_α radiation (0.71069 Å); data for **1** were collected on an Enraf–Nonius CAD4F diffractometer using Mo-K_α radiation (0.7093 Å) (Table 5). Structures were solved by a combination of Patterson search and direct methods (SHELX86) [39] and refined by full matrix least squares (SHELX76) [40]. Data were corrected for Lorentz and polarization effects but not for absorption. Hydrogen atoms were included in

Table 4

Complex	IR (cm^{-1}, hexane)	M.p. (°C)	Analysis (Found (calc.)(%))	
			C	H
1	1974, 1918	145 (dec)	70.1 (70.2)	6.00 (5.85)
2a	1978, 1925	oil	70.0 (69.8)	7.45 (7.33)
2b	1960, 1906	148–149	70.6 (70.2)	7.33 (7.36)
3	1974, 1914	oil	$[m^+]$	491.1790 (491.1793)
SeP(*o*-tolyl)$_3$	–	162–163	65.6 (65.8)	5.52 (5.48)

Table 5

	1	**2b**
	$C_{29}H_{29}FeO_2P$ triclinic	$C_{31}H_{39}FeO_2P$ orthorhombic
Space group	$P\bar{1}$	$P2_12_12_1$
Z	2	4
a	9.794(1) Å	9.156(2)
b	11.507(1)	14.299(3)
c	12.216(1)	21.483(5)
α	74.33(1)°	90°
β	73.32(1)	90
γ	70.45(1)	90
U	1219.40 Å^3	2812.59 Å^3
μ	6.53 cm^{-1}	5.61 cm^{-1}
$F(000)$	520	1132
Range	$2 < 2\theta < 48°$	$2 < 2\theta < 48°$
Reflections $I > 3\sigma(I)$	2620	1108
Variable parameters	163	170
Maximum shift/esd	< 0.001	< 0.001
R	5.36%	5.07%
R_w	4.74	5.66
Maximum excursion	0.22 e/Å^3	0.12 e/Å^3
Minimum excursion	−0.19	−0.12

calculated positions. The iron and phosphorus atoms and the CO groups were refined anisotropically. The atomic scattering factors for non-hydrogen and hydrogen atoms were taken from the literature [41–43]. Calculations were performed on VAX 11/785 or VAX 8700 computers. The drawings were generated using CHEM-X. Fractional atomic co-ordinates are listed in Table 6.

Table 6

Fractional atomic coordinates for complexes **1** and **2b**

Atom	*x*	*y*	*z*
Complex 1			
Fe1	0.19975(10)	0.63722(8)	0.15366(7)
P1	0.1466(2)	0.7935(1)	0.2544(1)
O1	0.3443(5)	0.4389(4)	0.3233(4)
O2	0.4580(5)	0.6703(4)	−0.0287(4)
C1	0.2859(7)	0.5207(6)	0.2593(5)
C2	0.3579(7)	0.6593(5)	0.0463(5)
C3	0.0545(7)	0.7368(5)	0.0363(5)
C4	−0.0131(7)	0.6669(5)	0.1391(5)
C5	0.0581(6)	0.5383(5)	0.1602(5)
C6	0.1876(7)	0.4959(6)	0.0787(5)
C7	0.1954(7)	0.5438(5)	−0.0497(5)
C8	0.1134(7)	0.6824(5)	−0.0739(5)
C9	0.2114(6)	0.9337(5)	0.1767(5)
C10	0.2298(7)	1.0214(5)	0.2277(5)
C11	0.2855(7)	1.1196(6)	0.1551(5)
C12	0.3197(7)	1.1339(6)	0.0356(5)
C13	0.2996(7)	1.0501(5)	−0.0155(5)
C14	0.2460(6)	0.9507(5)	0.0542(5)
C15	0.1878(7)	1.0211(6)	0.3570(5)
C16	0.2233(6)	0.7434(5)	0.3875(5)
C17	0.3788(7)	0.6986(5)	0.3798(5)
C18	0.4277(7)	0.6565(5)	0.4845(5)
C19	0.3318(7)	0.6587(6)	0.5907(6)
C20	0.1817(8)	0.7047(6)	0.5984(6)
C21	0.1282(7)	0.7467(5)	0.4962(5)
C22	0.4928(7)	0.7000(5)	0.2681(5)
C23	−0.0548(6)	0.8628(5)	0.3058(5)
C24	−0.1501(7)	0.7915(5)	0.3788(5)
C25	−0.3029(7)	0.8514(6)	0.4058(5)
C26	−0.3607(8)	0.9743(6)	0.3616(5)
C27	−0.2697(7)	1.0448(6)	0.2901(5)
C28	−0.1167(7)	0.9895(5)	0.2630(5)
C29	−0.0955(7)	0.6530(5)	0.4290(5)
Complex 2b			
Fe1	0.56030(21)	−0.02583(12)	0.27858(7)
P1	0.4486(4)	0.0408(2)	0.3603(1)
O1	0.6695(13)	−0.1771(9)	0.3576(6)
O2	0.3219(14)	−0.1157(9)	0.2126(5)
C1	0.6242(16)	−0.1169(10)	0.3260(6)
C2	0.4095(17)	−0.0766(10)	0.2402(6)
C3	0.7025(17)	−0.0658(11)	0.2041(7)
C4	0.7664(18)	−0.0017(10)	0.2440(7)
C5	0.7005(17)	0.0844(10)	0.2572(6)
C6	0.5592(17)	0.1053(8)	0.2318(6)
C7	0.5274(18)	0.1059(11)	0.1614(6)
C8	0.6365(17)	0.0551(11)	0.1219(7)
C9	0.6536(17)	−0.0465(10)	0.1376(6)
C10	0.2906(15)	0.1164(9)	0.3446(5)
C11	0.2387(14)	0.1834(8)	0.3880(6)
C12	0.1177(15)	0.2352(10)	0.3775(6)
C13	0.0449(18)	0.2244(10)	0.3220(6)

Table 6 (continued)

Atom	x	y	z
Complex 2b			
C14	0.0934(16)	0.1618((10)	0.2782(7)
C15	0.2122(14)	0.1104(9)	0.2881(6)
C16	0.3891(12)	−0.0390(9)	0.4247(5)
C17	0.3277(16)	0.0135(10)	0.4836(5)
C18	0.3152(16)	−0.0547(9)	0.5373(6)
C19	0.2291(21)	−0.1461(13)	0.5187(8)
C20	0.2808(19)	−0.1899(11)	0.4613(7)
C21	0.2984(16)	−0.1229(9)	0.4041(6)
C22	0.5789(14)	0.1174(7)	0.4023(5)
C23	0.5812(17)	0.2132(9)	0.3937(6)
C24	0.6911(15)	0.2677(9)	0.4227(6)
C25	0.7960(17)	0.2253(9)	0.4578(6)
C26	0.7940(18)	0.1310(10)	0.4669(7)
C27	0.6850(15)	0.0790(10)	0.4398(5)
C28	0.4614(23)	−0.0716(14)	0.5704(9)
C29	0.1005(21)	−0.1935(12)	0.3391(8)
C30	0.1558(16)	−0.1064(10)	0.3665(6)
C31	0.0308(20)	−0.0591(12)	0.4003(8)

References and notes

1 For quantitative data on the binding of P(*o*-tolyl)$_3$ see: (a) L.M. Ounapu, J.A. Mosbo, J.M. Risley and B.N. Stornhoff, J. Organomet. Chem., 194 (1980) 337; (b) S. Matsumoto and S. Kawaguchi, Bull. Chem. Soc. Jpn., 54 (1981) 1704; (c) P. Bandyopadhyay, P.K. Mascharak and A. Chakravorty, Inorg. Chim. Acta, 45 (1980) L219; (d) A.M. Bond, R. Colton, D. Dakternieks, K.W. Hanck and M. Svestka, Inorg. Chem., 22 (1983) 236; (e) Y. Nakamura, K. Maruya and T. Mizoroki, J. Organomet. Chem., 104 (1976) C5; (f) L.E. Manzer and C.A. Tolman, J. Am. Chem. Soc., 97 (1975) 1955; (g) K. Sanshiro and A. Shibue, Organometallics, 4 (1985) 684; (h) C.A. Tolman, J. Am. Chem. Soc., 92 (1970) 2956; (i) K.W. Barnett and T.G. Pollmann, J. Organomet. Chem., 69 (1974) 413.

2 For recent applications of metal–P(*o*-tolyl)$_3$ complexes in catalysis, see: (a) H.X. Zhang, F. Guibe and G. Balavoine, J. Org. Chem., 55 (1990) 1987; (b) G.T. Crisp and A.I. O'Donoghue, Synth. Commun., 19 (1989) 1745; (c) B.M. Trost, S. Matsubara and J.J. Caringi, J. Am. Chem. Soc., 111 (1989) 8745; (d) M. Kakimoto, M. Yoneyana and Y. Imai, Polym. Mater. Sci. Eng., 60 (1989) 98; (e) W. Hartmann and H. Singer, J. Mol. Catal., 48 (1988) 81; (f) E. Farnetti, J. Kaspar, R. Spogliarich and M. Graziani, J. Chem. Soc., Dalton Trans., (1988) 947; (g) R. Grigg, P. Stevenson and T. Warakun, Tetrahedron, 44 (1988) 2049; (h) W.J. Thompson, J.H. Jones, P.A. Lyle and E.J. Thies, J. Org. Chem., 53 (1988) 2052; (i) J.J. Bozzell and C.E. Vogt, J. Am. Chem. Soc., 110 (1988) 2655.

3 J.M. Brown and P.L. Evans, Tetrahedron, 44 (1988) 4905.

4 J.A.S. Howell, Adv. Dyn. Stereochem., 1 (1985) 111.

5 J.A. Chudek, G. Hunter, R.L. Mackay, P. Kremmingher, K. Schlogl and W. Weissensteiner, J. Chem. Soc., Dalton Trans., (1990) 2001; (b) G. Hunter, T.J. Weakley and W. Weissensteiner, ibid., (1987) 1545.

6 Such gearing has been predicted from molecular mechanics studies: C.E. du Plooy, C.F. Marcus, L. Carton, R. Hunter, J.C.A. Boeyens and N.J. Coville, Inorg. Chem., 28 (1989) 3855.

7 For an example of correlated rotation of η^2-ethene and η^6-benzene on an Os_3 cluster, see: D. Braga, F. Grepiani, B.F.G. Johnson, J. Lewis and M. Mortinelli, J. Chem. Soc., Dalton Trans., (1990) 1847.

8 (a) K. Mislow, Chemtracts–Organic Chemistry, 2 (1989) 151; (b) U. Berg, T. Liljefors, C. Roussel and J. Sandstrom, Acc. Chem. Res., 18 (1985) 80.

9 (a) A.J. Pearson, Adv. Met.-Org. Chem., 1 (1989) 1; (b) G.R. Stephenson, R.P. Alexander, C. Morley and P.W. Howard, Philos. Trans. R. Soc. London, Ser. A, 326 (1988) 545; (c) R. Gree, Synthesis, (1989) 341.

10 (a) A.J. Birch and L.F. Kelly, J. Organomet. Chem., 286 (1985) C5; (b) C.M. Adams, A. Hafner, M. Koller, A. Marcuzzi, R. Preivo, I. Solana, B. Vincent and W. von Phillipsborn, Helv. Chim. Acta, 12 (1989) 1658.
11 T.S. Cameron and B. Dahlen, J. Chem. Soc., Perkin Trans. II, (1975) 1737.
12 A.J. Pearson and P.R. Raithby, J. Chem. Soc., Dalton Trans., (1981) 884.
13 C.A. Tolman, Chem. Rev., 77 (1977) 313. The cone angle values quoted for P(o-tolyl)$_3$ and PPh_3 are 194 and 145°, respectively.
14 The exo_3 conformation was modelled using CHEM-X [15] by addition of an Fe atom to P(o-tolyl)$_3$ generated from the literature coordinates [11] (Fe–P = 2.28 Å). Half-cone angle values for the three phenyl rings were measured using a Van der Waals radius for the methyl group of 2.0 Å and θ calculated using the formula $\theta = \frac{2}{3}\Sigma_{i=1}^{3}\theta_i/2$. The value of 184° represents the average for the two crystallographically independant P(o-tolyl)$_3$ molecules in the unit cell. The θ value of 160° for the exo_2 conformation was calculated in the same way from the Fe–P(o-tolyl)$_3$ fragment of **1** using a Van der Waals radius of 1.2 Å for the C6-hydrogen of the down ring.
15 CHEM-X, program developed and distributed by Chemical Design Limited, Oxford, England.
16 J.A.S. Howell, G. Walton, M.-C. Tirvengadum, A.D. Squibb, M.G. Palin, P. McArdle, D. Cunningham, Z. Goldschmidt, H. Gottlieb and G. Strul, J. Organomet. Chem., 401 (1991) 91.
17 (a) D. Wormsbacher, F. Edelmann, D. Kaufmann, U. Behrens and A. de Meijere, Angew. Chem., Int. Ed. Engl., 20 (1981) 696; (b) G.A. Sim, D.I. Woodhouse and G.R. Knox, J. Chem. Soc., Dalton Trans., (1979) 629; (c) K.D. Karlin, M.P. Moiran, M. Kustyn, P.L. Dahlstrom, J. Zubieta and P.R. Raithby, Cryst. Struct. Commun., 11 (1982) 1945.
18 Line shape analysis was performed using the EXCHANGE program, R.E.D. McLung, University of Alberta.
19 $\Delta G^{\ddagger}$ values were calculated using the equation

$$k = \frac{\kappa k_B T}{h} e^{-\Delta G^{\ddagger}/RT}$$

A value of $\kappa = 1$ was applied to the CH_2 resonances and $\kappa = 0.333$ to the CH_3 resonances since for the latter process, magnetization is being transferred from a symmetrical intermediate not to one but to three methyl signals, each at the fitted rate [20]. Errors in $\Delta G^{\ddagger}$ were calculated using the equation [21] $(\sigma\Delta G^{\ddagger}/\Delta G^{\ddagger})^2 = [\ln(k_B T/hk)]^{-2}(\sigma_k/k)^2 + (\sigma_T/T)^2$ using the σ_k values in Table 3 and a σ_T value of ±3 K. Values of $\Delta H^{\ddagger}$ and $\Delta S^{\ddagger}$ were derived from a plot of $\Delta G^{\ddagger}/T$ aginst $1/T$. The 95% confidence limits for $\Delta H^{\ddagger}$ and $\Delta S^{\ddagger}$ were calculated according to reference 20, p. 115.
20 J. Sandstrom, Dynamic NMR Spectroscopy, Academic Press, New York, 1982, pp. 93–94.
21 L.M. Jackman and F.A. Cotton, Dynamic Nuclear Magnetic Resonance Spectroscopy, Academic Press, New York, 1975, pp. 76–77.
22 J.A.S. Howell, A.D. Squibb, Z. Goldschmidt, H.E. Gottlieb, A. Almadhoun and I. Goldberg, Organometallics, 9 (1990) 80.
23 Previous reports on the variable temperature NMR spectra of SeP(o-tolyl)$_3$ have been inconsistent: (a) R.A. Shaw, M. Woods, T.S. Cameron and B. Dahlen, Chem. Ind., (1971) 151; (b) R.A. Shaw, M. Woods, W. Egan and J. Jacobus, ibid., (1973) 532. We are preparing a full report on the series XP(o-tolyl)$_3$ (X = O, S, Se).
24 (a) D. Gust and K. Mislow, J. Am. Chem. Soc., 95 (1973) 1535; (b) M.R. Kates, J.D. Andose, P. Finocchiaro, D. Gust and K. Mislow, ibid., 97 (1975) 1772; (c) E.J. Hapern and K. Mislow, ibid., 89 (1967) 5224; (d) J.P. Hummel, E.P. Zurbach, E.N. DiCarlo and K. Mislow, ibid., 98 (1976) 7480.
25 Either A/B or A/C flipping yields the one-up, two-down conformer. Evidence on the relative energy of this conformation is lacking, but one may note the one-up, two-down structure of SP(m-tolyl)$_3$ [26].
26 T.S. Cameron, K.D. Howlett, R.A. Shaw and M. Woods, Phosphorus, 3 (1973) 71.
27 There is a similar correlation of helical chirality with metal chirality in $CpFe(CO)(PPh)_3COR$ complexes: S.G. Davies, Pure Appl. Chem., 60 (1988) 13.
28 Calculations [24b] indicate a higher energy for the three-ring relative to the two-ring-flip.
29 Turnstile rotation results in exchange of the axial CO resonance of the major diastereoisomer with the basal CO resonance of the minor diastereoisomer and *vice versa*. Assuming a value of J(P–CO(axial)) of ca. 4 Hz (unresolved at −100 °C due to resonance overlap), and a diastereoisomer ratio of 2.5 : 1, there is good agreement between calculated and observed averaged resonances for **2b** at +20 °C (Table 1). The much closer chemical shifts and coupling constants for **2a** reflect the smaller

diastereoisomer ratio, while the smaller averaged coupling constants for 3 reflect the significant population of the axial phosphine isomer [16].
30 A.J. Pearson, S.L. Kole and T. Ray, J. Am. Chem. Soc., 106 (1984) 6060.
31 A.M. Aguiar, C.J. Morrow, J.D. Morrison, R.E. Burnett and W.F. Masler, J. Org. Chem., 41 (1976) 1545.
32 (a) J.A.S. Howell, A.D. Squibb, G. Walton, P. McArdle and D. Cunningham, J. Organomet. Chem., 319 (1985) C45; (b) J.A.S. Howell, M.C. Tirvengadum, A.D. Squibb, G. Walton, P. McArdle and D. Cunningham, ibid., 347 (1988) C5.
33 (a) P. Salvadori, P. Pertici, F. Marchetti, R. Lazzaroni and M.A. Bennett, J. Organomet. Chem., 370 (1989) 155; (b) G. Jaouen, J.A.S. Howell, M.C. Tirvengadum, P. McArdle and D. Cunningham, ibid., 370 (1989) 51.
34 K. Kau, Y. Kai, N. Yasuoka and N. Kasai, Bull. Chem. Soc. Jpn., 50 (1977) 1051.
35 J.A.S. Howell and M.J. Thomas, J. Chem. Soc., Dalton Trans., (1983) 1401.
36 S.V. Ley, C.M.R. Low and A.D. White, J. Organomet. Chem., 302 (1986) C13.
37 J.D. Morrison and W.F. Masler, J. Org. Chem., 39 (1974) 270.
38 D.W. Allen, I.W. Nowell and B.F. Taylor, J. Chem. Soc., Dalton Trans., (1985) 2505.
39 G.M. Sheldrick, SHELX86, A Computer Program for Crystal Structure Determination, University of Göttingen, 1986.
40 G.M. Sheldrick, SHELX76, A Computer Program for Crystal Structure Determination, University of Cambridge, 1976.
41 D.T. Cromer and J.B. Mann, Acta Crystallogr., Sect. A, 24 (1968) 321.
42 D.T. Cromer and D.J. Liberman, J. Chem. Phys., 53 (1970) 1891.
43 R.F. Stewart, E.R. Davidson and W.T. Simpson, J. Chem. Phys., 42 (1965) 3175.